NACA

RESEARCH MEMORANDUM

DATA FROM FLOW-FIELD SURVEYS BEHIND A LARGE-SCALE

THIN STRAIGHT WING OF ASPECT RATIO 3

By William T. Evans

Ames Aeronautical Laboratory
Moffett Field, Calif.

NATIONAL ADVISORY COMMITTEE
FOR AERONAUTICS
WASHINGTON
June 23, 1958

NATIONAL ADVISORY COMMITTEE FOR AERONAUTICS

RESEARCH MEMORANDUM

DATA FROM FLOW-FIELD SURVEYS BEHIND A LARGE-SCALE

THIN STRAIGHT WING OF ASPECT RATIO 3

By William T. Evans

SUMMARY

Limited flow-field surveys were made behind a large-scale thin straight wing of aspect ratio 3, both alone and in combination with a body and vertical tail. The wing section was a modified double wedge, 4.2 percent thick. The surveys were made at geometric angles of attack from 8° to 30°, at a free-stream dynamic pressure of 20 pounds per square foot. The Reynolds number, based on the mean aerodynamic chord of the wing, was approximately 8.5×10^6.

The surveys indicated a region of high downwash angles, low dynamic pressures, and rough flow, that extended higher above the wing chord plane, and farther aft, with increasing angle of attack beyond the stall. It is argued that the growth of such a region with angle of attack is probably typical for thin straight wings.

INTRODUCTION

An exploratory force study in the Ames 40- by 80-foot wind tunnel of a model with a thin straight wing and a high-mounted horizontal tail revealed extreme instability and severe loss of longitudinal-control effectiveness above the stall. As a result, a longitudinal trim point which was relatively insensitive to tail incidence occurred at a very high angle of attack.

To study the source of this condition, surveys of flow direction and dynamic pressure were made behind the wing. The results of these surveys are presented herein, and some qualitative inferences are drawn.

NOTATION

A   aspect ratio

b   wing span, ft

c   wing chord, ft

$\bar{c}$ mean aerodynamic chord, ft

C_L lift coefficient

C_m pitching-moment coefficient, moment center at $\frac{\bar{c}}{4}$

C_{m_T} tunnel-wall-effect correction to C_m

i_t incidence of horizontal tail, deg

q_l local dynamic pressure, lb/sq ft

q_∞ free-stream dynamic pressure, lb/sq ft

R   Reynolds number, based on $\bar{c}$

x   longitudinal coordinate (streamwise), from $\frac{\bar{c}}{4}$, ft

y   lateral coordinate, from plane of symmetry, ft

z   vertical coordinate (perpendicular to free stream), from
        extended wing chord plane, ft

α corrected angle of attack, deg

α_T tunnel-wall-effect correction to α_u, deg

α_u uncorrected (geometric) angle of attack, deg

ϵ downwash angle, deg

η fraction of wing semispan

MODEL, APPARATUS, AND TESTS

    A sketch of the complete model is shown in figure 1. The wing
geometry is given in figure 2, which also shows the locations of the
survey planes. The surveys in the x-z plane at $\eta = 0.28$ were made

above and behind the wing-body-vertical-tail configuration at geometric
angles of attack of 22° and 30°. No corrections were applied to the
measured flow directions. To augment these surveys, brief tuft and
smoke-flow studies were made. The surveys in the y-z plane were made
behind the "wing alone" (i.e., the wing plus supporting beam, as indi-
cated in fig. 2) at geometric angles of attack of 8°, 12°, 16°, and 22°.
Measured downwash angles were corrected for tunnel-wall effect and for
the effect of the survey apparatus, as described in reference 1, which
includes a description of the apparatus itself. All surveys were made
at a dynamic pressure of 20 pounds per square foot.

Force data were obtained with each of the horizontal tails indicated
in figure 1, as well as without a horizontal tail. For some data, ply-
wood fins as indicated in figure 1 were added to the model. Dynamic
pressures ranged from 5-1/2 to 20 pounds per square foot, and are indi-
cated in the figures. The corresponding range of Reynolds numbers,
based on the mean aerodynamic chord, was 4.5 to 8.5x10⁶. Corrections
for tunnel-wall effects, when applied, are indicated in the figures.

RESULTS AND DISCUSSION

Basic Force Data

Lift and pitching-moment curves are presented in figure 3 for the
model with each of the horizontal tails, as well as without a horizontal
tail. The pitching-moment variation of the model with either tail on
was unstable above an angle of attack of 16°, a trim point occurred at
a high angle of attack, and the tail contribution nearly disappeared at
the highest angles of attack.

To indicate the effect of tail incidence, exploratory runs with
the tail of aspect ratio 4 were made, and the pitching-moment results
are presented in figure 4. (For these runs the fins indicated in fig-
ure 1 were on the model. Also, no corrections were applied to the angle
of attack, because of the unknown effect of the presence of the survey
apparatus just downstream of the test section.) A severe loss of tail
effectiveness at the highest angles of attack is evident.

In all runs with a horizontal tail, extreme buffeting of the tail
was observed at the highest angles of attack.

Results of Flow-Field Surveys

Surveys in the x-z plane above and behind the wing-body-vertical-
tail configuration.- The results of these surveys are shown in figure 5.

For each angle of attack ($\alpha_u = 22^\circ$ and 30°), the flow field above and behind the wing is indicated by means of local flow vectors, with lengths proportional to the local dynamic pressure. The shaded area in each case indicates the region in which flow vectors could not be reliably determined because of such factors as flow direction, low dynamic pressure, or rough flow. Broken arrows within this area indicate estimated flow directions (but not dynamic pressures) from brief tuft and smoke-flow studies. These broken arrows also indicate, very roughly, the region of separated flow (which does not coincide with the shaded area).

As would be expected from the force data, large downwash angles and low dynamic pressures are indicated at the horizontal-tail position. These evidently result from the large region of separated flow which trails downstream from the wing, and which grows with angle of attack.

Surveys in the y-z plane behind the wing alone.- The results of these surveys are shown in figures 6 and 7 as profiles of downwash angle and dynamic pressure, respectively. The profiles show a rapid increase in downwash angle and loss of dynamic pressure in the region of the high tail as angle of attack is increased. This pattern is consistent with the results of the x-z surveys; however, comparison with the latter for $\alpha_u = 22^\circ$ shows that the effect of the body was to cause considerably greater values of downwash at the intersection of the two survey planes.

Discussion

Because the investigation was exploratory, discussion will be limited to observations of a qualitative nature.

Thin-airfoil stall in two-dimensional flow is characterized by the onset of flow separation from the leading edge at a low angle of attack, and the subsequent continuous growth of the region of separated flow with increasing angle of attack (ref. 2). While two-dimensional data are confined to angles of attack that do not extend far beyond the angle for maximum lift, it is reasonable to suppose that the separated region simply continues to grow, to indefinitely high angles of attack, in much the manner suggested by figure 5. In short, it seems likely that the stalled flow behind any thin straight wing would be dominated by this presumed two-dimensional flow pattern, except in the vicinity of the tip vortices. The inference is that there is a region above and behind any such wing in which the placement of a horizontal tail will result in a severe loss of longitudinal stability and control effectiveness through a particular range of angles of attack.

In references 3 and 4 additional data are given for small-scale models ($R = 2\times10^6$) with wings of the same plan form and type of section as in the present model. In reference 3 both force and downwash data

are included, while the data of reference 4 are confined to measurements of downwash angle. While these data will not be discussed here, it is considered that they support the qualitative inference drawn above.

CONCLUDING REMARKS

It is considered that the basic flow pattern behind a stalled wing of the type tested results in a region of high downwash angles, low dynamic pressure, and rough flow that extends higher above the wing-chord plane, and farther aft, with increasing angle of attack. It follows that a tail of moderate span placed so as to be within this region for certain angles of attack cannot be expected to maintain good stability and control effectiveness through that range of angles of attack.

Ames Aeronautical Laboratory
    National Advisory Committee for Aeronautics
        Moffett Field, Calif., April 17, 1958

REFERENCES

1. Tolhurst, William H., Jr.: Downwash Characteristics and Vortex-Sheet Shape Behind a 63° Swept-Back Wing-Fuselage Combination at a Reynolds Number of 6.1×10^6. NACA TN 3175, 1954. (Supersedes NACA RM A52J08)

2. McCullough, George B., and Gault, Donald E.: Example of Three Representative Types of Airfoil-Section Stall at Low Speed. NACA TN 2502, 1951.

3. Delany, Noel K., and Hayter, Nora-Lee F.: Low-Speed Investigation of a 0.16-Scale Model of the X-3 Airplane - Longitudinal Characteristics. NACA RM A50G06, 1950.

4. Hopkins, Edward J., and Sorensen, Norman E.: Downwash Survey Behind Two Low-Aspect-Ratio Variable-Incidence Wings in Combination With Three Different Size Fuselages at a Mach Number of 0.25. NACA RM A55A07, 1955.

Figure 1.- Sketch of the complete model.
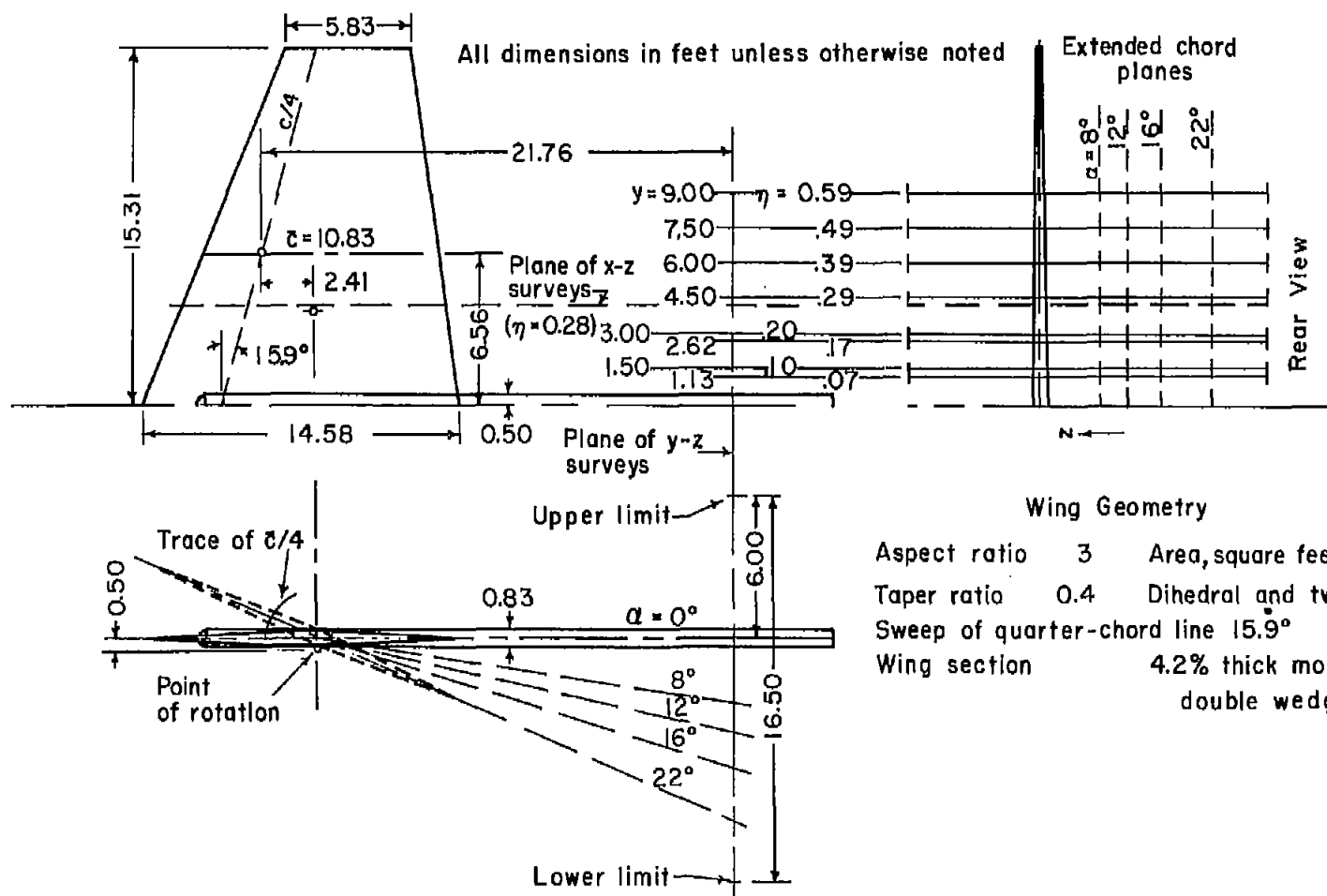
All dimensions in feet
unless otherwise noted

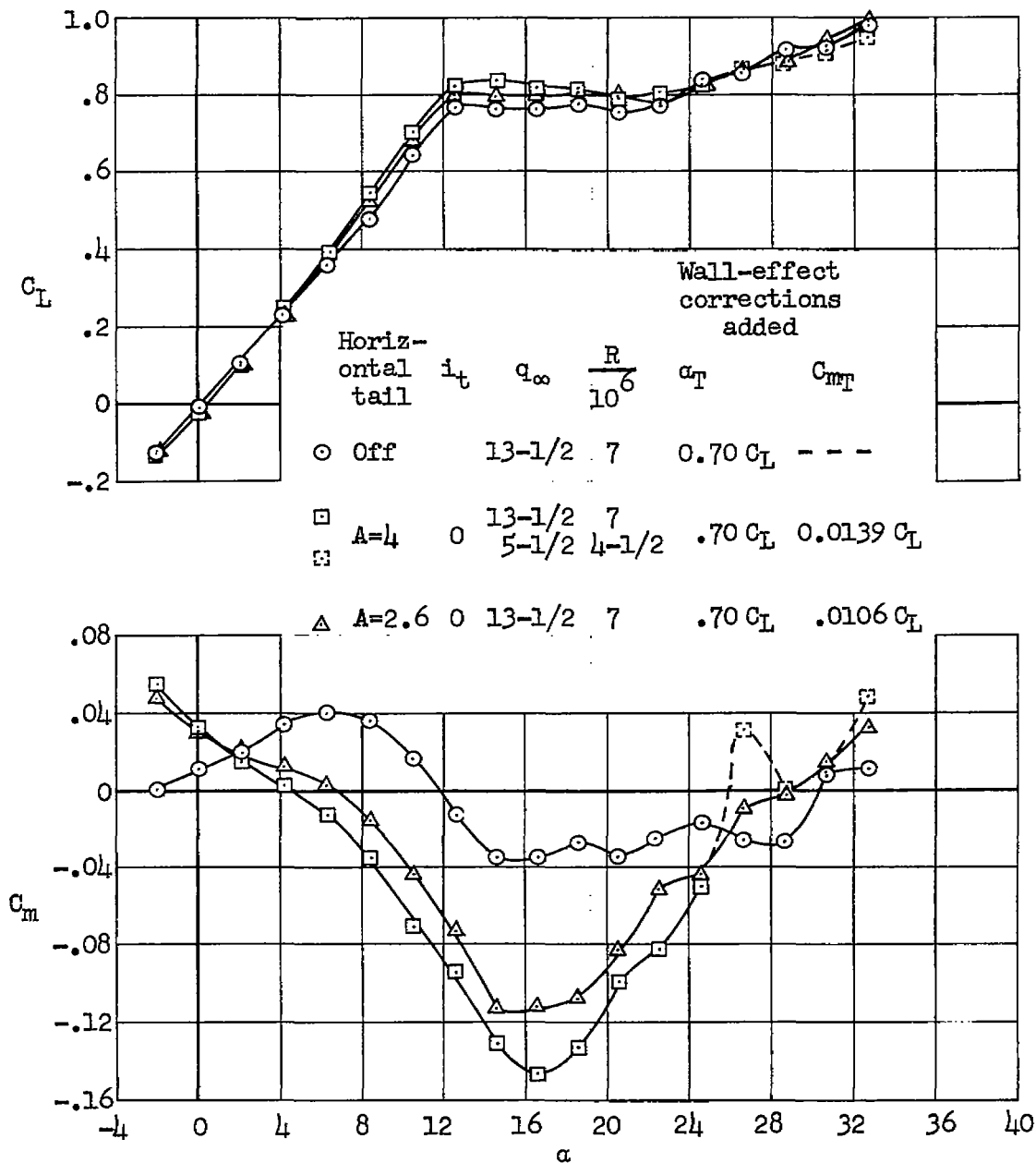Figure 2.- Wing geometry and locations of flow-field surveys.

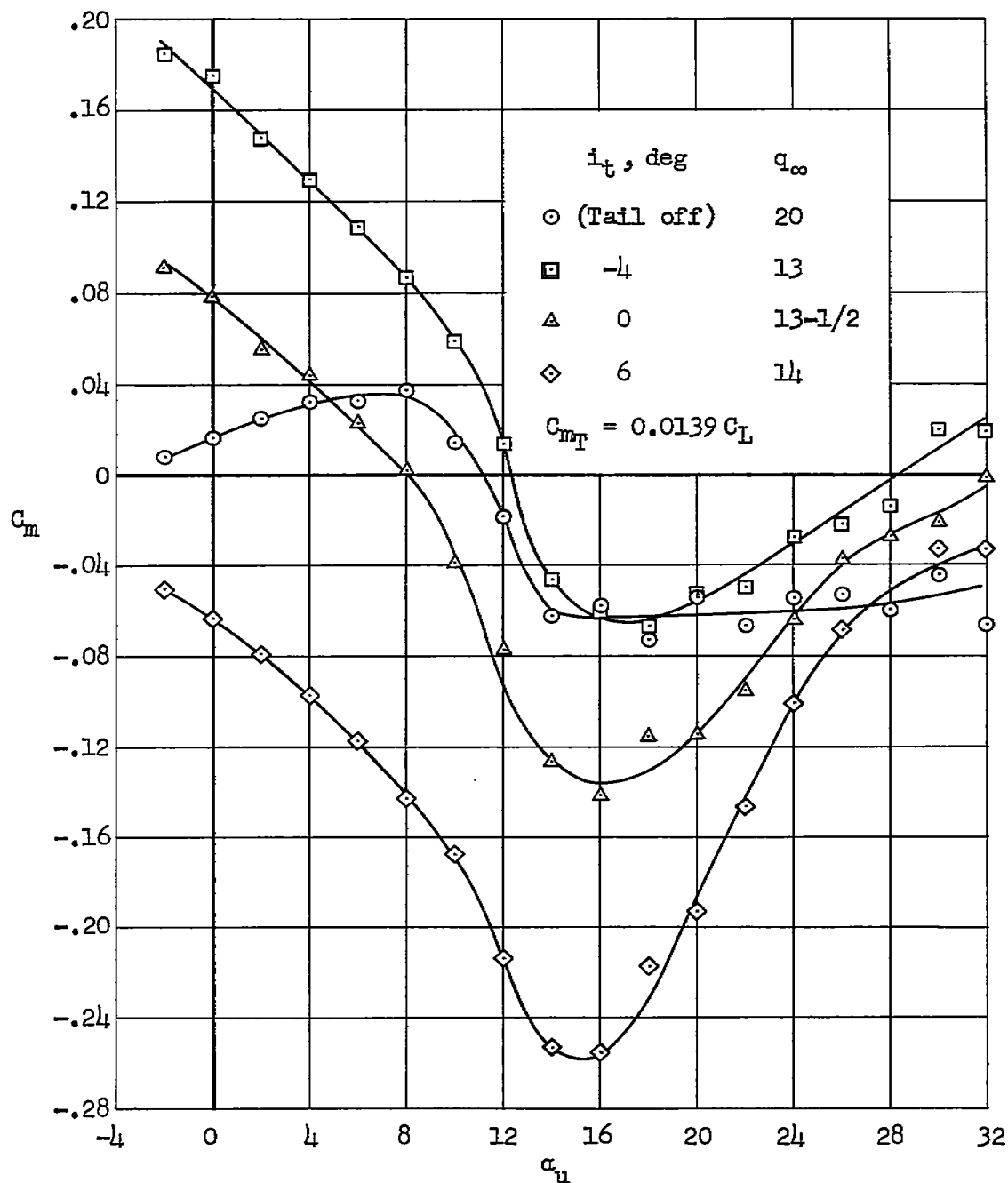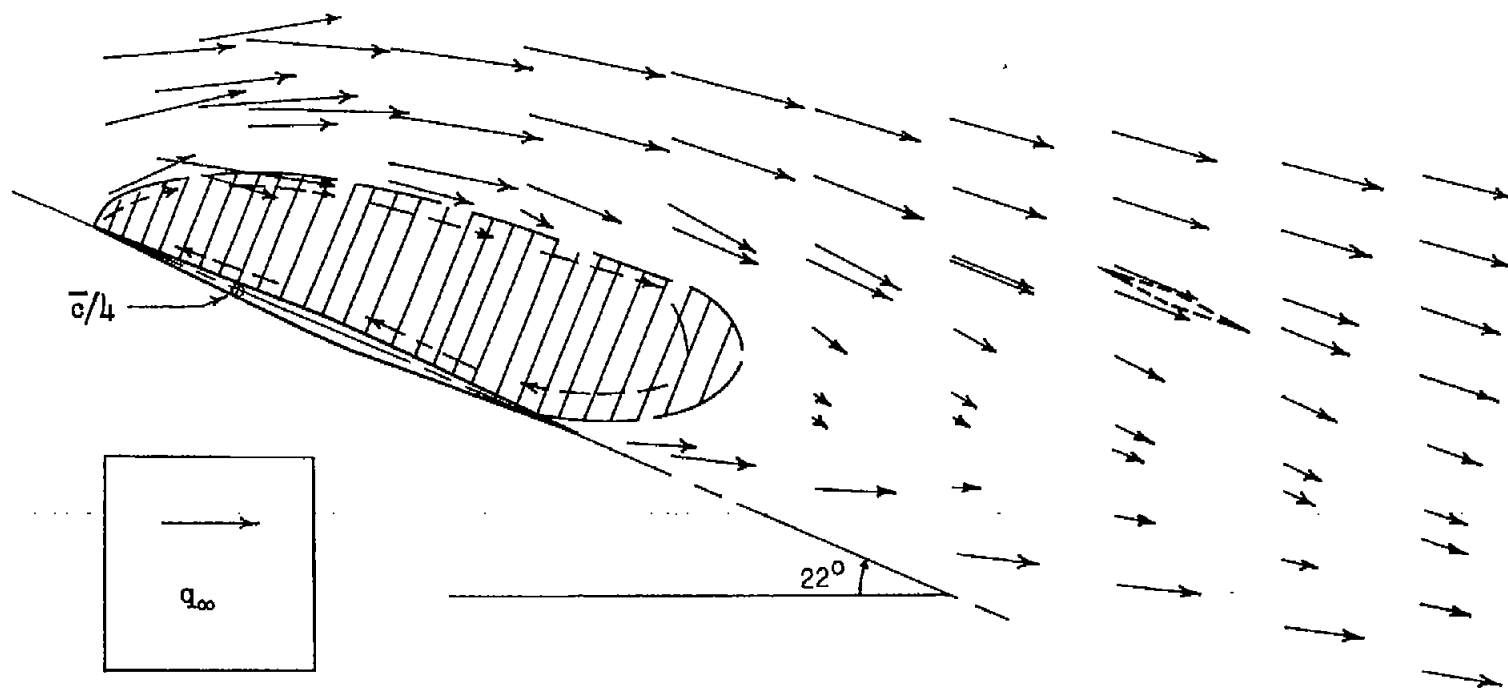Figure 3.- Longitudinal characteristics of the model with and without a horizontal tail.
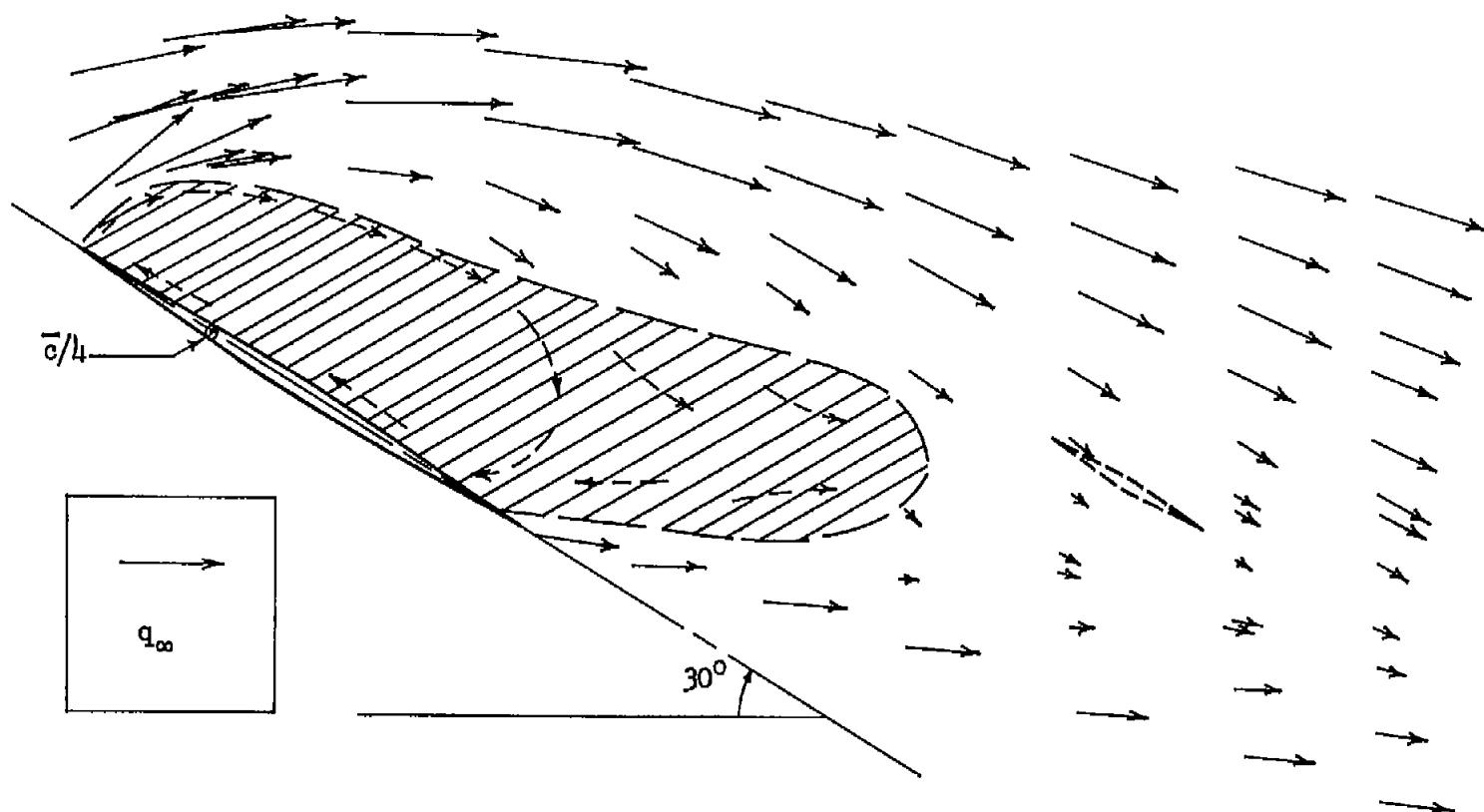
Figure 4.- Effect of tail incidence on the pitching-moment characteristics
of the model with fins; aspect-ratio-4 tail.

(a) $\alpha_u = 22^\circ$

Figure 5.- Dynamic-pressure vectors in the x-z plane at $\eta = 0.28$.
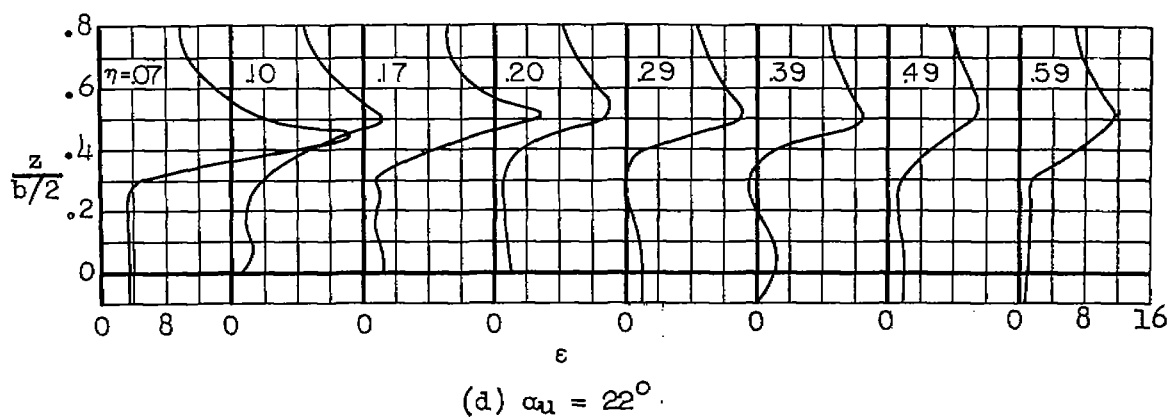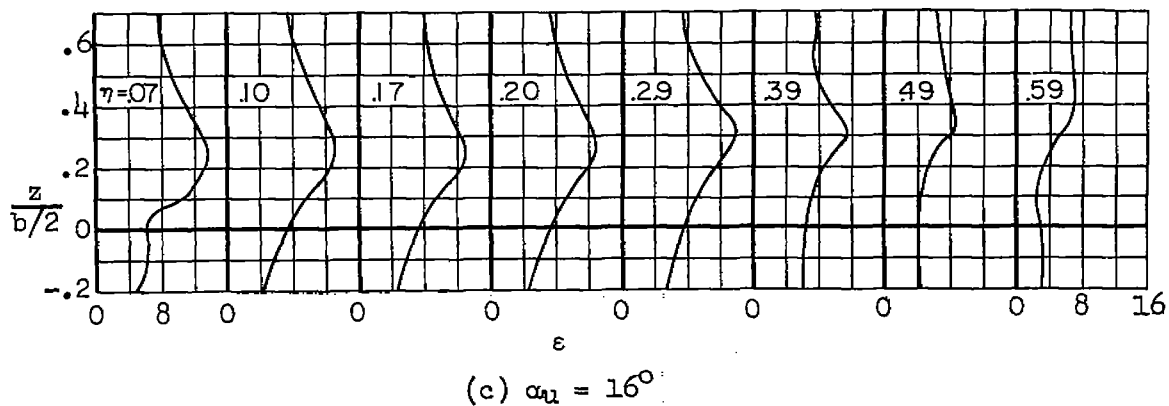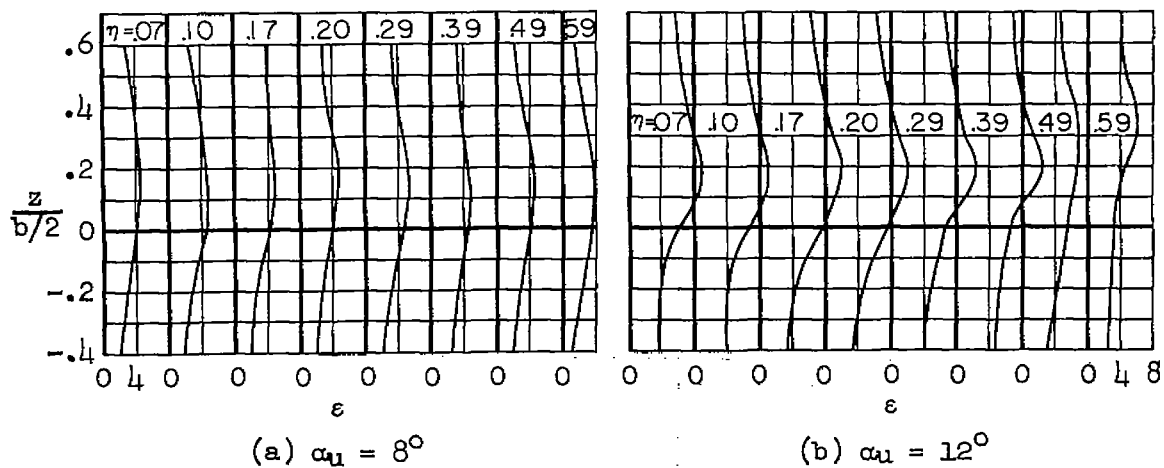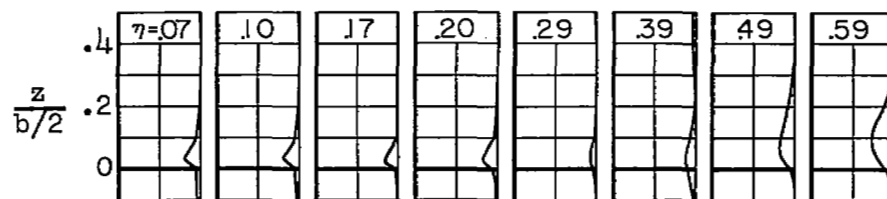
(b) $\alpha_u = 30^\circ$

Figure 5.- Concluded.

(a) $\alpha_u = 8°$

(b) $\alpha_u = 12°$

(c) $\alpha_u = 16°$

(d) $\alpha_u = 22°$

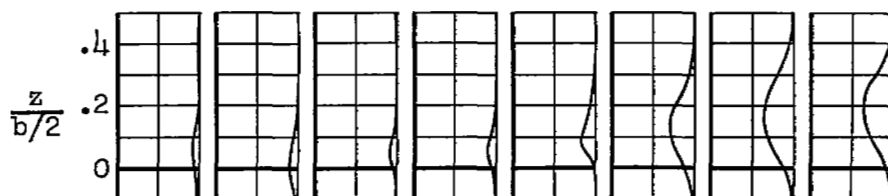Figure 6.- Profiles of downwash angle measured in the y-z survey plane behind the wing alone.
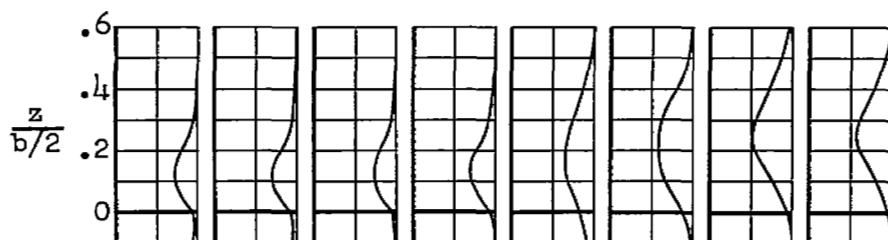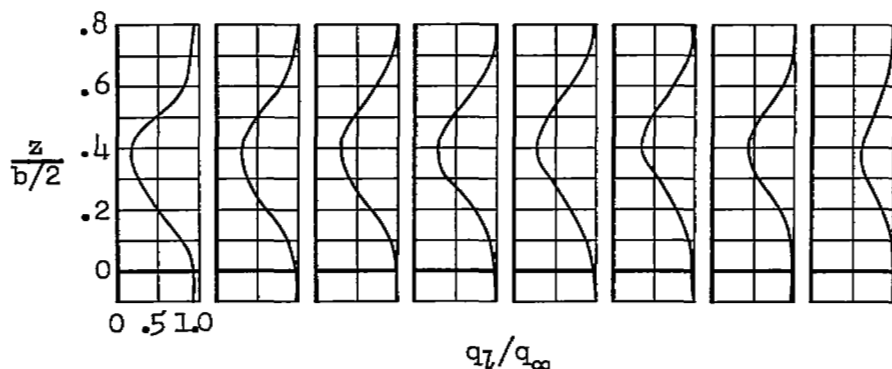
(a) $\alpha_u = 8^\circ$

(b) $\alpha_u = 12^\circ$

(c) $\alpha_u = 16^\circ$

(d) $\alpha_u = 22^\circ$

Figure 7.- Profiles of dynamic-pressure ratio in the y-z survey plane behind the wing alone.